

Configurational entropy-induced phase transition in spinel $LiMn_2O_4$

Wei Hu(胡伟), Wen-Wei Luo(罗文崴), Mu-Sheng Wu(吴木生), Bo Xu(徐波), and Chu-Ying Ouyang(欧阳楚英)
Citation: Chin. Phys. B, 2022, 31 (**9**): 098202. DOI: 10.1088/1674-1056/ac6863
Journal homepage: http://cpb.iphy.ac.cn; http://iopscience.iop.org/cpb

What follows is a list of articles you may be interested in

Electron density distribution of $LiMn_2O_4$ cathode investigated by synchrotron powder x-ray diffraction

Tongtong Shang(尚彤彤), Dongdong Xiao(肖东东), Qinghua Zhang(张庆华), Xuefeng Wang(王雪锋), Dong Su(苏东), and Lin Gu(谷林)
Chin. Phys. B, 2021, 30 (**7**): 078202. DOI: 10.1088/1674-1056/abf347

Quantum simulations with nuclear magnetic resonance system

Chudan Qiu(邱楚丹), Xinfang Nie(聂新芳), and Dawei Lu(鲁大为)
Chin. Phys. B, 2021, 30 (**4**): 048201. DOI: 10.1088/1674-1056/abe299

Adsorption of propylene carbonate on the $LiMn_2O_4$ (100) surface investigated by DFT + *U* calculations

Wei Hu(胡伟), Wenwei Luo(罗文崴), Hewen Wang(王鹤文), and Chuying Ouyang(欧阳楚英)
Chin. Phys. B, 2021, 30 (**3**): 038202. DOI: 10.1088/1674-1056/abd77e

Suppressing transition metal dissolution and deposition in lithium-ion batteries using oxide solid electrolyte coated polymer separator

Zhao Yan(闫昭), Hongyi Pan(潘弘毅), Junyang Wang(汪君洋), Rusong Chen(陈汝颂), Fei Luo(罗飞), Xiqian Yu(禹习谦), Hong Li(李泓)
Chin. Phys. B, 2020, 29 (**8**): 088201. DOI: 10.1088/1674-1056/ab9610

A low cost composite quasi-solid electrolyte of LATP, TEGDME, and LiTFSI for rechargeable lithium batteries

Jie Huang(黄杰), Jia-Yue Peng(彭佳悦), Shi-Gang Ling(凌仕刚), Qi Yang(杨琪), Ji-Liang Qiu(邱纪亮), Jia-Ze Lu(卢嘉泽), Jie-Yun Zheng(郑杰允), Hong Li(李泓), Li-Quan Chen(陈立泉)
Chin. Phys. B, 2017, 26 (**6**): 068201. DOI: 10.1088/1674-1056/26/6/068201

Configurational entropy-induced phase transition in spinel $LiMn_2O_4$

Wei Hu(胡伟)[1,2], Wen-Wei Luo(罗文崴)[1], Mu-Sheng Wu(吴木生)[1], Bo Xu(徐波)[1], and Chu-Ying Ouyang(欧阳楚英)[1,†]

[1] *Department of Physics, Laboratory of Computational Materials Physics, Jiangxi Normal University, Nanchang* 330022, *China*
[2] *School of Ecology and Environment, Yuzhang Normal University, Nanchang* 330103, *China*

(Received 1 March 2022; revised manuscript received 6 April 2022; accepted manuscript online 20 April 2022)

The spinel-type $LiMn_2O_4$ is a promising candidate as cathode material for rechargeable Li-ion batteries due to its good thermal stability and safety. Experimentally, it is observed that in this compound there occur the structural phase transitions from cubic ($Fd\bar{3}m$) to tetragonal ($I4_1/amd$) phase at slightly below room temperature. To understand the phase transition mechanism, we compare the Gibbs free energy between cubic phase and tetragonal phase by including the configurational entropy. Our results show that the configurational entropy contributes substantially to the stability of the cubic phase at room temperature due to the disordered Mn^{3+}/Mn^{4+} distribution as well as the orientation of the Jahn–Teller elongation of the $Mn^{3+}O_6$ octahedron in the the spinel phase. Meanwhile, the phase transition temperature is predicted to be 267.8 K, which is comparable to the experimentally observed temperature. These results serve as a good complement to the experimental study, and are beneficial to the improving of the electrochemical performance of $LiMn_2O_4$ cathode.

Keywords: configurational entropy, $LiMn_2O_4$, phase transition, Jahn–Teller distortion

PACS: 82.47.Aa, 81.05.Hd, 82.20.Ej **DOI:** 10.1088/1674-1056/ac6863

1. Introduction

Lithium-ion batteries (LIBs) have been widely used in many fields due to their excellent electrochemical performances, such as potable electronic devices, electric vehicles, and smart grid storage over the last few decades.[1–4] The performances of LIBs, *i.e.*, energy density, capacity, rate capability, and cycling life, are closely related to the cathode materials. The spinel-type compound, $LiMn_2O_4$, is considered as one of the most promising materials with good electrochemical performance in LIBs due to its good thermal stability and safety, low cost, environmental benign, high energy density, *etc.*[5–8] At ambient temperature, the crystal structure of $LiMn_2O_4$ belongs to the cubic $Fd\bar{3}m$ space group,[9] where lithium ions are located at the tetrahedral 8*a* sites, manganese ions at the octahedral 16*d* sites and oxygen ions at the 32*e* sites.[10] Since the average valence of manganese ions in $LiMn_2O_4$ is 3.5, the same numbers of Mn^{3+} and Mn^{4+} ions are randomly distributed at the 16*d* sites. However, upon cooling a first-order phase transition occurs at a temperature of ca 280 K from cubic to tetragonal ($I4_1/amd$) phase,[11–16] which hinders this compound from being put into practical application. Yamada and Tanaka[11] observed the splitting of reflections at low temperature by using thermal analysis and powder x-ray diffraction. This indicates that $LiMn_2O_4$ undergoes phase transition at low temperature. Yamaguchi *et al.*[15] investigated an x-ray absorption fine structure (XAFS) of $LiMn_2O_4$, further confirmed the fact of the phase transition at low temperature, and reported that a phase transition occurs in the vicinity of 280 K by differential scanning calorimetric (DSC) measurement. Piszora *et al.*[17] found that this phase transition is related to the Jahn–Teller effect and partial charge ordering of Mn^{3+} and Mn^{4+} ions, but the detailed mechanism has not been reported. The potential profile test of $LiMn_2O_4$ by Abiko *et al.*[18] found that $LiMn_2O_4$ has an additional low voltage plateau and spinel powder is pulverized by lattice stress at low temperatures. Chung and Kim[19,20] reported that the presence of the tetragonal phase of $LiMn_2O_4$ particle due to a Jahn–Teller effect is one of the reasons for capacity fade by using *in situ* laser probe beam deflection technique. Therefore, in order to avoid the performance degradation caused by low temperature phase transition and promote the wide application of $LiMn_2O_4$ cathode, it has become an urgent topic to study phase transition mechanism of $LiMn_2O_4$ at the low temperature.

As is well known, Jahn–Teller (JT) distortion exists in the MnO_6 octahedron for Mn^{3+} ions, but not for Mn^{4+} ions. Generally speaking, the JT distortion gives rise to the lowering of the symmetry and the observed cubic phase at room temperatures seems not reasonable, as the MnO_6 framework is tetragonally distorted. Considering the randomly distributed Mn^{3+} ions in the lattice, it is also possible that the orientation of the JT distortion is random, namely, the elongation of the $Mn^{3+}O_6$ octahedron is randomly distributed along the *x*-, *y*-, and *z*-axis directions. That is to say, the configuration of $LiMn_2O_4$ may be related to the distribution of Mn^{3+} ions and the elongation direction of the $Mn^{3+}O_6$ octahedron. In this way, the cubic structures can also be exit due to the JT effect of the $Mn^{3+}O_6$ octahedron. Furthermore, Piszora[17] reported that the phase

†Corresponding author. E-mail: cyouyang@jxnu.edu.cn

© 2022 Chinese Physical Society and IOP Publishing Ltd

transition is induced by the JT distortion and partial charge ordering of Mn^{3+} and Mn^{4+} ions with temperature decreasing, indicated by using powder synchrotron radiation diffraction. On the basis of this analysis, we speculate that the structural phase transition from cubic to tetragonal phase is closely related to the configurational entropy originating from the distribution of the Mn^{3+} and Mn^{4+} ions and the orientation of the JT distortion direction of $Mn^{3+}O_6$ octahedron.

To further verify and understand the mechanism of phase transition, we study the transition between cubic phase and tetragonal phase by including the configurational entropy contribution to the Gibbs free energy from the thermodynamic point of view in this work. The ground state energy is obtained by using the first-principles calculations. It is shown that the average ground state energy of the cubic $LiMn_2O_4$ (disordered phase) is higher than that of the tetragonal one (more ordered phase) at a temperature of 0 K. When the configurational entropy is included, the Gibbs free energy of the cubic phase lowers with the temperature increasing and finally the phase transition from cubic phase to tetragonal phase happens at a temperature of 267.8 K, which is close to the experimental result.[11,15,18]

2. Computational method

To optimize the structures and obtain the ground state energy values of different structures and phases, we performed density functional theory (DFT) calculations by using the Vienna *ab-initio* simulation package (VASP).[21–23] The method of the projected augmented wave (PAW)[24,25] pseudopotentials was used to describe the ion–electron interactions. The electron exchange and correlation functional were treated within the spin polarized generalized gradient approximation (GGA) in the form of the Perdew–Burke–Ernzerh (PBE) functional.[26] A cutoff energy of 500 eV was selected for the plane wave basis set. In order to account for the strong onsite Coulomb repulsion of Mn-3d electrons, the GGA+U method[27,28] was adopted, which could accurately predict the electronic structures of transition metal complexes. Based on previous reports, the effective U value for d-orbital of Mn ions was set to be 4.5 eV.[29,30] The Monkhorst–Pack scheme[31] with $3 \times 3 \times 3$ k-points sampling mesh was used for the integration in the irreducible Brillouin zone. The atomic positions and the lattice parameters were fully relaxed, and the final force was less than 0.01 eV/Å for each atom. The calculation workflow was managed by the high-throughput computational platform for battery materials.[1]

3. Results and discussion

The spinel-type $LiMn_2O_4$ consists of 32 O, 16 Mn, and 8 Li atoms in a conventional unit cell as shown in Fig. 1. According to the crystal field theory, the Mn-3d orbital will undergo an energy level splitting, producing a double degenerate e_g ($d_{x^2-y^2}$, d_{z^2}) and a triple degenerate t_{2g} (d_{xy}, d_{yz}, d_{xz}) orbitals under an octahedral crystal field as shown in Fig. 2.

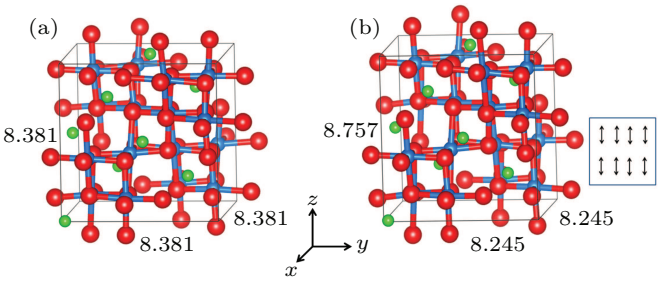


Fig. 1. Ball and stick models of (a) cubic and (b) tetragonal $LiMn_2O_4$, along with lattice parameters (in units of Å). Comparing with cubic phase, the lattice c of tetragonal phase expands, while lattices a and b shrink. Arrows in the inset indicate the Jahn–Teller distortion direction of Mn^{3+} ions. The red, green, and blue spheres represent O, Li, and Mn atoms, respectively.

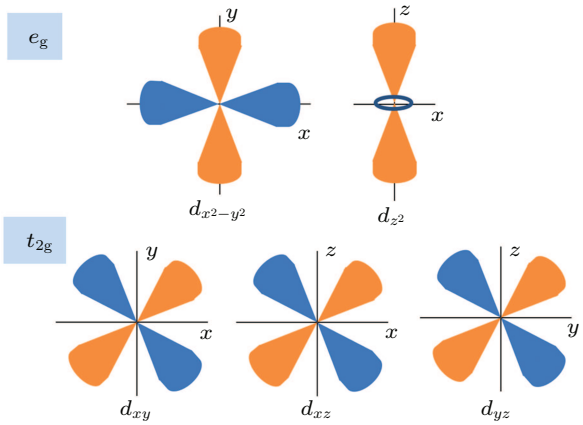


Fig. 2. Schematic diagram of energy level splitting for Mn-3d orbital under an octahedral field.

The projected density of states and corresponding electronic configuration of the Mn^{3+} ion and Mn^{4+} ion in the $LiMn_2O_4$ are shown in Fig. 3. As can be seen, the electronic configuration of the Mn-3d state of the Mn^{3+} ion and Mn^{4+} ion are $t_{2g}^3e_g^1$ and $t_{2g}^3e_g^0$, respectively.[32,33] Since the e_g orbital is directly facing the ligand atom, it is subjected to larger Coulomb repulsion, resulting in the JT distortion of Mn^{3+} ion in MnO_6 octahedron, forming four short and two long Mn–O bonds in the $Mn^{3+}O_6$ octahedron as shown in Table 1. For Mn^{4+} ions, the e_g orbital is not occupied by electrons, so the bond lengths in the $Mn^{4+}O_6$ octahedron are approximately equal. Considering the equivalence of the x, y, and z directions, the orientation of the JT distortion can be in any direction. If the orientation is randomly distributed along the x, y, and z directions, the crystal structure behaves as cubic phase. In contrast, if the orientation of the JT distortion is unique in one direction, say, along the z direction, the lattice constant c will be larger than that of a and b and thus the crystal structure acts as tetragonal phase. Experimentally, Chung and Kim[19] also observed that the lattice c expands and the lattice a shrinks during the phase transition from cubic to tetragonal phase for

$LiMn_2O_4$. In order to study the phase transition, we need to construct and simplify these two models.

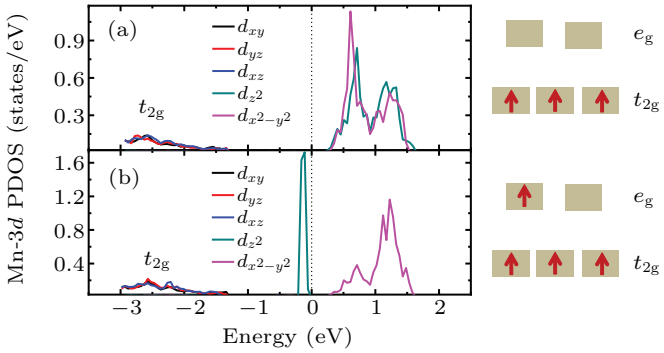


Fig. 3. Projected densities of states and corresponding electronic configurations of Mn-3d orbitals for (a) Mn^{4+} and (b) Mn^{3+} in $LiMn_2O_4$, with Fermi levels set to be 0 eV.

Table 1. The Mn–O bond length in MnO_6 octahedron, where long bonds are highlighted.

	Bond length (Å)					
Mn^{4+}–O	1.927	1.929	1.932	1.966	1.968	1.975
Mn^{3+}–O	1.977	1.985	1.948	1.977	2.184	2.187

As mentioned above, there are 16 Mn ions in the unit cell of the spinel $LiMn_2O_4$. Among them, half of these Mn ions are trivalent Mn ions, and the others are tetravalent ones. On the other hand, the JT effects of Mn^{3+} ions have three possible distortion directions (x, y, and z directions). Therefore, the total number of possible Mn^{3+} distributions and $Mn^{3+}O_6$ orientation configurations in the unit cell of $LiMn_2O_4$ is $C_{16}^{8} \times 3^8$. For each configuration, the ground state energy of the unit cell can be different, and in this work we use an average over several typical models we employed, which will greatly reduce the happenchance of a single configuration. Owing to the vast number of possible configurations and our limited computational resource, we select only 12 configurations (as shown in Fig. 4) to optimize their structures and calculate the ground state energy. The optimized lattice parameters and the corresponding energy values for the selected 12 configurations are listed in Table 2. The average values of the lattice parameters and the ground state energy values of the cubic phase are also listed in Table 3, which are considered to be the lattice parameters and ground state energy of the cubic phase in this work. Likewise, the $LiMn_2O_4$ in the tetragonal phase is also dealt with by this procedure. Owing to the sole direction of the JT distortion (z axis in our calculations) for the tetragonal phase, the degree of freedom of the JT distortion is not considered.

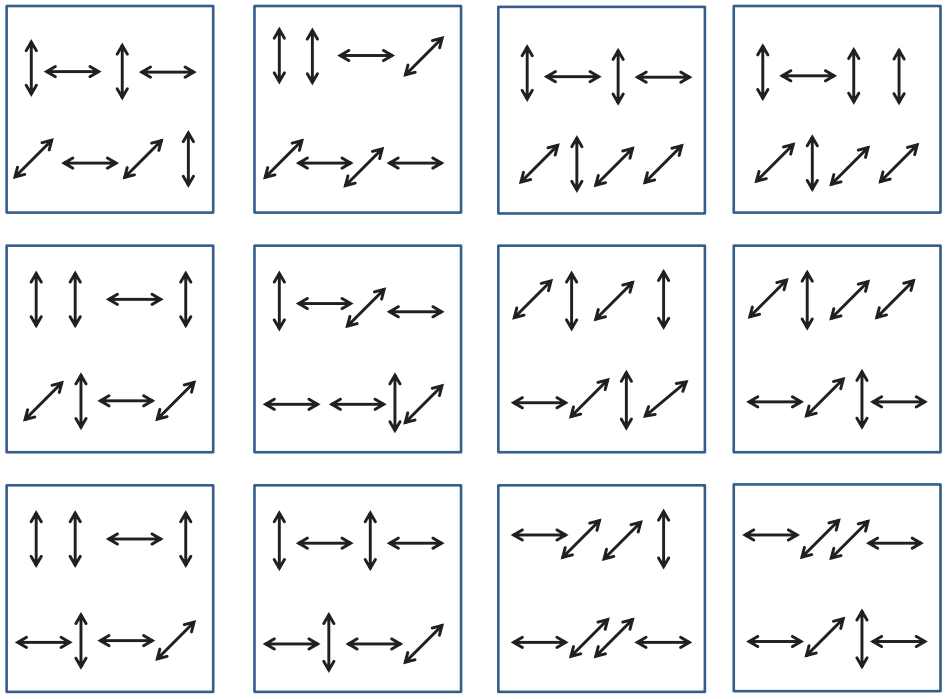


Fig. 4. Jahn–Teller distortion directions of the eight $Mn^{3+}O_6$ for the selected 12 cubic configurations, with horizontal, vertical, and slanted arrows representing the directions along the x, z, and y axes, respectively.

Table 2. Lattice parameters and total energy values of selected 12 cubic configurations.

Model	Lattice parameter (Å)	Total energy (eV)	Model	Lattice parameter (Å)	Total energy (eV)
M1	8.397	–374.630	M7	8.367	–374.734
M2	8.361	–374.714	M8	8.378	–374.327
M3	8.403	–374.680	M9	8.376	–374.365
M4	8.407	–374.602	M10	8.381	–374.764
M5	8.371	–374.405	M11	8.375	–374.754
M6	8.363	–374.720	M12	8.393	–374.788

Table 3. Lattice parameters and average ground state energy values of $LiMn_2O_4$ unit cell in cubic and tetragonal phases. Herein, the lattice parameters and total energy values are average values of various configurations calculated.

	Cubic	Tetragonal
a (Å)	8.381 (8.25exp[16,17])	8.245
b (Å)	8.381	8.245
c (Å)	8.381	8.757
c/a	1	1.062 (1.004 exp.[34])
Total energy (eV)	–374.623	–374.802

Therefore, only the configurations with the different Mn^{3+} distributions are considered. Here, three different configurations are used to calculate the average values of lattice parameters and the ground state energy values as listed in Table 3. Likewise, these average values are taken as the average values of the lattice parameters and ground state energy values of the tetragonal phase in this work.

As is well known, the Gibbs free energy G can be expressed as $G = H - TS$, where H denotes the enthalpy, and S is the entropy. For solid phase, the contribution of pressure to H can be ignored. As a result, the change of the Gibbs free energy is influenced by the environment through the entropy. Therefore, only the configurational entropy is taken into account in this work. After the ground state energy is obtained, we need to determine the configurational entropy (S_{conf}), which is given as $S_{\text{conf}} = k_{\text{B}} \ln \Omega$, where Ω is the number of configurations, k_{B} represents the Boltzmann constant. Herein, it should be pointed out that the interaction between Mn ions is ignored. Therefore, for the cubic phase, $\Omega = C_{16}^{8} \cdot 3^{8}$, whereas for the tetragonal phase, $\Omega = C_{16}^{8}$. The Gibbs free energy as a function of temperature for the cubic phase and tetragonal phase are shown in Fig. 5. As can be seen, a crossover point at a temperature of 267.8 K can be found. When the temperature is higher than 267.8 K, the cubic phase is more stable than the tetragonal one. When the temperature decreases below 267.8 K, the transition from cubic phase to tetragonal phase is expected. This theoretically predicted phase transition temperature of about 267.8 K for $LiMn_2O_4$ from cubic to tetragonal phase is close to that observed experimentally ($\sim$ 280 K) by using x-ray absorption spectroscopy by Yamada and Tanaka,[11] Yamaguchi *et al.*,[15] and Abiko *et al.*[18] This also shows the important role of configurational entropy in the phase transition process.

Although the phase transition temperature obtained from our calculations is close to that from experiments, there are still some factors that we did not consider in this study. Firstly, the vibrational entropy induced by the finite temperature is not included in our model. This cannot be an important fact, for the difference in vibrational entropy between the cubic phase and tetragonal phase should be small and the bonding interactions are the same in the compound. Secondly, it is worth noting that the limited configurations chosen in our calculations also influences the accuracy of the ground state energy. Despite these, we believe that the introduction of configurational entropy can qualitatively reveal the nature of transition between cubic phase and tetragonal phase, which is helpful for us to understand the phase transition of the spinel-type $LiMn_2O_4$.

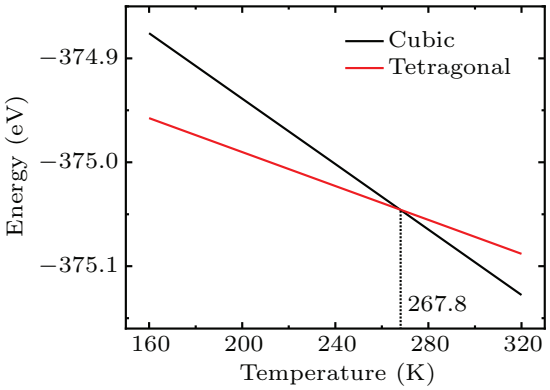


Fig. 5. Plot of Gibbs free energy *versus* temperature of $LiMn_2O_4$ unit cell for cubic phase and tetragonal phase. Herein, the ground state energy employed is average value of the corresponding configuration as shown in Table 3.

4. Conclusions

In this work, the phase transition of the spinel $LiMn_2O_4$ between cubic phase and tetragonal phase are studied through DFT calculations combined with thermodynamic analysis. The ground state energy is calculated through DFT for each configuration at zero temperature, while the entropy is evaluated through atomic configurational evaluation. It is found that the ground state energy of the cubic phase with the disordered JT distortion direction of the Mn^{3+} ion is higher than that of the tetragonal phase with the ordered orientation of the JT distortion. On the other hand, the configurational entropy of the cubic phase is higher than that of the tetragonal phase. As a result, the cubic phase is more stable at high temperatures while the tetragonal phase is more stable at relatively low temperature. The phase transition temperature is evaluated to be 267.8 K through combining the calculated total ground state energy with the configurational entropy, which is comparable to the experimental value. These findings help further understand the phase transition of $LiMn_2O_4$ at low temperature, and serve as a complement to experimental studies. In particular, the failure of $LiMn_2O_4$ cathode is more clearly recognized at low temperature, which helps broaden the application scope of $LiMn_2O_4$.

Acknowledgement

Project supported by the National Natural Science Foundation of China (Grant Nos. 12174162, 51962010, 12064015, and 12064014).

References

[1] He B, Chi S T, Ye A J, Mi P H, Zhang L W, Pu B W, Zou Z Y, Ran Y B, Zhao Q, Wang D, Zhang W Q, Zhao J T, Adams S, Avdeev M and Shi S Q 2020 *Sci. Data* **7** 151

[2] Cheng Y, Shu J, Xu L, Xia Y Y, Du L L, Zhang G and Mai L Q 2021 *Adv. Energy Mater.* **11** 2100026

[3] Shang Y, Chen N, Li Y, Chen S, Lai J, Huang Y, Qu W, Wu F and Chen R 2020 *Adv. Mater.* **32** 2004017

[4] Gao H, Yan Q, Xu P, Liu H, Li M, Liu P, Luo J and Chen Z 2020 *ACS Appl. Mater. Inter.* **12** 51546

[5] Song D, Ikuta H, Uchida T and Wakihara M 1999 *Solid State Ionics* **117** 151

[6] Tarascon J, Wang E, Shokoohi F, Mckinnon W and Colson S 1991 *J. Electrochem. Soc.* **138** 2859

[7] Thackeray M M, David W I F, Bruce P G and Goodenough J B 1983 *Mater. Res. Bull.* **18** 461

[8] Jiang Q Q, Xu L, Ma Z L and Zhang H 2015 *Appl. Phys. A* **119** 1069

[9] Sugiyama J, Tamura T and Yanauchi H 1995 *J. Phys.: Condens. Matter* **7** 9755

[10] Wickham D G and Croft W J 1958 *J. Phys. Chem. Solids* **7** 351

[11] Yamada A and Tanaka M 1995 *Mater. Res. Bull.* **30** 715

[12] Yamada A 1996 *J. Solid State Chem.* **122** 160

[13] Mukai K, Uyama T and Yamada I 2019 *ACS Omega* **4** 6459

[14] Oikawa K, Kamiyama T, Izumi F, Chakoumakos B C, Ikuta H, Wakihara M, Li J and Matsui Y 1998 *Solid State Ionics* **109** 35

[15] Yamaguchi H, Yamada A and Uwe H 1998 *Phys. Rev. B* **58** 8

[16] Rodríguez-Carvajal J, Rousse G, Masquelier C and Hervieu M 1998 *Phys. Rev. Lett.* **81** 4660

[17] Piszora P 2004 *J. Alloys Compd.* **382** 112

[18] Abiko H, Mitsuhiro Hibino M and Kudo T 2000 *Solid State Ionics* **135** 115

[19] Chung K Y and Kim K B 2002 *J. Electrochem. Soc.* **149** A79

[20] Chung K Y and Kim K B 2004 *Electrochim. Acta* **49** 3327

[21] Kresse G and Hafner J 1994 *Phys. Rev. B* **49** 14251

[22] Kresse G and Furthmüller J 1996 *Phys. Rev. B* **54** 11169

[23] Kresse G and Furthmuüller J 1996 *Comput. Mater. Sci.* **6** 15

[24] Blochl P E 1994 *Phys. Rev. B* **50** 17953

[25] Kresse G and Joubert D 1999 *Phys. Rev. B* **59** 1758

[26] Perdew J P, Bruke K and Emzerhof M 1996 *Phys. Rev. Lett.* **77** 3865

[27] Anisimov V I, Zaanen J and Andersen O K 1991 *Phys. Rev. B* **44** 943

[28] Anisimov V I, Aryasetiawan F and Lichtenstein A I 1997 *J. Phys.: Condens. Matter* **9** 767

[29] Zheng L M, Wang H W, Luo M, Wang G Q, Wang Z Q and Ouyang C Y 2018 *Solid State Ionics* **320** 210

[30] Xiao R J, Li H and Chen L Q 2012 *Chem. Mater.* **24** 4242

[31] Monkhorst H J and Pack J D 1976 *Phys. Rev. B* **13** 5188

[32] Ouyang C Y, Du Y L, Shi S Q and Lei M S 2009 *Phys. Lett. A* **373** 2796

[33] Ouyang C Y, Shi S Q and Lei M S 2009 *J. Alloys Compd.* **474** 370

[34] Piszora P, Paszkowicz W, Baehtz C and Wolska E 2004 *J. Alloys Compd.* **382** 119